

## A CRASH AVOIDANCE SYSTEM BASED UPON THE COCKROACH ESCAPE RESPONSE CIRCUIT

Chun-Ta Chen and Roger D. Quinn  
Mechanical and Aerospace Engineering  
and  
Roy E. Ritzmann  
Biology  
Case Western Reserve University  
Cleveland, Ohio 44106

### *Abstract*

A crash avoidance system for automobiles is developed based upon a distributed network of artificial neurons that mimic the neural organization of the escape system in the American cockroach. The cockroach escape circuit is shown to be an excellent source of inspiration for the development of a collision avoidance system. The crash avoidance system is implemented in an artificial neural network which is trained off-line, but then is shown to produce real-time performance. A collision avoidance scheme which makes use of a crash alarm strategy is developed for training the neural network. A dynamic model of a four-wheeled vehicle with front wheel steering and realistic performance constraints is used to test the crash avoidance system. Simulation results show that the well-trained neural network causes successful, reflexive crash avoidance behaviors in a dynamic environment without a priori information.

### 1. INTRODUCTION

Many researchers have focused on obstacle avoidance for autonomous vehicles. In the classical approach to the problem, called the artificial potential field method<sup>1</sup>, a robot is assumed to travel in a field of imaginary forces, where obstacles are considered to exert repulsive forces and the goal applies an attractive force on the robot. Much of the recent work in obstacle avoidance was inspired by the layered control systems and subsumption architecture developed by Brooks<sup>2</sup>. Brooks' robots follow a bottom-up engineering approach with the focus being on interaction with the environment and task-achieving behaviors. Borenstein and Koren<sup>3</sup> proposed a two-dimensional Cartesian histogram grid as a world model for a real-time obstacle avoidance method for mobile robots. Arkin<sup>4</sup> defined control actions with independent behaviors called schemas and implemented a variation of the potential fields method in a mobile robot. Less literature is devoted to the problem of avoidance of obstacles which are moving on unknown paths<sup>5</sup>. Perception, decision-making, motion planning, and real-time control play crucial roles in this kind of crash avoidance.

In this paper, a crash avoidance system for four-wheeled vehicles is developed based upon a distributed network of artificial neurons that mimic the neural organization of the escape system in the American cockroach. The goal of a crash avoidance system is to faithfully detect a threat from within numerous benign stimuli, identify where the threat is coming from and evoke appropriate avoidance maneuvers in the context of the vehicle's internal state and its environment. The system must do all of this in a very short period of time. These are also the goals of escape systems found in animals.

The cockroach escape circuit accurately identifies rapidly accelerating wind stimuli as arising from predators. Wind information is gathered by mechanoreceptive hairs and is conducted to the thorax by giant interneurons. There it is integrated by a distributed population of interneurons, called type A thoracic interneurons ( $TI_A$ 's). The  $TI_A$ 's direct turning movements away from the lunging predator via both direct and indirect connections to the leg motor neurons. All of this is accomplished in approximately 60ms<sup>6</sup>.

A crash avoidance system that only factored in the most immediate threat might cause a collision with another threat such as a wall or another passing vehicle. The cockroach solves this problem by incorporating context dependence into its system. In addition to monitoring wind inputs from predators, the  $TI_A$ s receive input from exteroceptive cues such as antennal contact, auditory responses and ambient light and proprioceptive cues on the state and position of the legs. The distributed network of  $TI_A$ s interprets the data on wind direction in the context of everything else the cockroach is experiencing at the moment of the attack. The context dependent nature of the escape system permits a very short reaction time because a suitable response need not be planned at the time of a particular threat, but is continuously updated based upon the animal's physiological state and its environment. Thus, the cockroach escape circuit satisfies all of the requirements for a successful crash avoidance system.

The neural circuit that comprises the cockroach escape system has been previously documented by intracellular analysis and modeled on a computer as a distributed network of artificial neurons<sup>7,8</sup>. In this paper, a crash avoidance system is developed for four-wheeled vehicles based upon this circuit and tested in simulation. The crash avoidance circuit incorporates sensory structures that detect approaching threats and then evokes appropriate avoidance maneuvers, e.g. turning, braking and accelerating.

## 2. DYNAMICS AND CONTROL OF A FOUR WHEELED VEHICLE

The cornering kinematics of a simplified four-wheel vehicle with front wheel steer (FWS) are shown in Figure 1 where *c.m.* is the center of mass of the vehicle. The four wheels have equal radii  $r_w$ . The wheel base is  $2a$  and the track is  $2b$ . The mass of the vehicle is denoted by  $m$  and the moment of inertia about the  $z$ -axis is  $I_z$ . The steering angle  $\phi$  can be considered as the steering angle of a "virtual wheel" which is attached to the middle point between wheel 1 and wheel 2.  $I_s$  is the moment of inertia of the steering system. The Ackerman steering constraint is enforced so that the front wheels do not scrub when the vehicle is turning. The sideslip angle  $\alpha$  is defined as the angle between the tangential velocity direction of the *c.m.* and the vehicle forward heading direction<sup>9</sup>,  $2 \tan \alpha = \tan \phi$ . The velocity of the *c.m.*,  $\underline{v}$  and the time derivative of the yaw rate,  $\dot{\theta}$ , can be expressed, respectively, as

$$\underline{v} = \dot{s} \begin{bmatrix} \cos \alpha \\ \sin \alpha \end{bmatrix}; \quad \ddot{\theta} = \frac{1}{a} (\dot{s} \sin \alpha + s \dot{\alpha} \cos \alpha) \quad (1a,b)$$

where  $s$  is the displacement of the *c.m.* along the path of the vehicle.

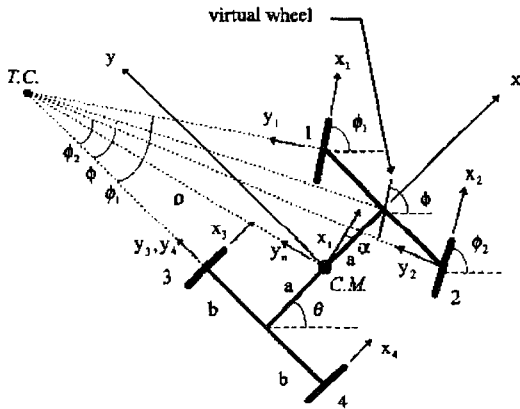


Figure 1: Four wheeled vehicle with front wheel steering.

Assuming that the applied torque on each wheel is  $\tau_i = 1/4\tau_e$ ,  $i=1 \sim 4$ , where  $\tau_e$  is the total applied engine/braking torque and  $\tau_s$  is the applied torque on the steering wheel, the equations of motion of the vehicle can be expressed as<sup>10</sup>

$$D_s \ddot{\underline{z}}_s + \underline{G}_s(\underline{z}_s, \dot{\underline{z}}_s) = \underline{u}; \quad \underline{z}_s = \begin{bmatrix} s \\ \phi \end{bmatrix}; \quad \underline{u} = \begin{bmatrix} \tau_e \\ \tau_s \end{bmatrix} \quad (2a-c)$$

where  $D_s$  and  $\underline{G}_s$  are the inertia matrix and a column of gyroscopic terms, respectively.

The variables  $s$  and  $\phi$  are coupled under the respective control inputs  $\tau_e$  and  $\tau_s$ . If the steering angle  $\phi$  is a constant, then the dynamical equations are reduced to one degree-of-freedom which can be expressed as

$$\underline{D}_{s1} \ddot{s} = \underline{u} \quad (3)$$

where  $\underline{D}_{s1}$  is the first column of  $D_s$ .

Realistic limits on engine torque and wheel/ground friction can be formulated into bounds on the tangential speed  $\dot{s}$  and tangential acceleration  $\ddot{s}$ . The engine/braking torque, the speed and the steering angle must satisfy

$$\tau_{\min} \leq \tau_e \leq \tau_{\max}; \quad 0 \leq \dot{s} \leq \dot{s}_{\max}; \quad \phi_{\min} \leq \phi \leq \phi_{\max} \quad (4a,b,c)$$

The subscripts 'max' and 'min' denote the maximum and minimum value of a quantity, respectively. The minimum steering angle  $\phi_{\min}$  is equal to  $-\phi_{\max}$ .

Feedback linearization can be applied in a straightforward manner to this class of nonlinear dynamical systems to achieve the desired local stabilization. A control law referred to as the computed torque method may be expressed as

$$\underline{u} = D_s \ddot{\underline{z}}_d + \underline{G}_s(\underline{z}_s, \dot{\underline{z}}_s) \quad (5)$$

Eq. (5) is substituted into Eqs. (2a), the nonlinearity is canceled and the closed-loop dynamics are obtained as

$$\ddot{\underline{z}}_s = \ddot{\underline{z}}_d - K_1(\dot{\underline{z}}_s - \dot{\underline{z}}_d) - K_2(\underline{z}_s - \underline{z}_d) \quad (6a,b)$$

The subscript 'd' represents the desired action for crash avoidance, and the  $(2 \times 2)$  gain matrices  $K_1$  and  $K_2$  may be selected so that the system has independent actuators. This can be achieved by assigning the gain matrices  $K_1, K_2$  as diagonal matrices:  $K_1 = \text{diag}[k_1^s, k_1^\phi]$  and  $K_2 = \text{diag}[k_2^s, k_2^\phi]$ . Therefore, Eq. (6a) is decoupled into independent error dynamics

$$\ddot{\underline{e}} + K_1 \dot{\underline{e}} + K_2 \underline{e} = 0 \quad (7)$$

where  $\underline{e} = \underline{z}_s - \underline{z}_d = [e_s, e_\phi]^T = [s - s_d, \phi - \phi_d]^T$  is composed of the scalar path error and steering angle

error. The elements of the gain matrices are chosen based on eigenvalue assignments to attain the desired state as soon as possible to avoid a potential crash.

### 3. BIOLOGICALLY-INSPIRED CRASH AVOIDANCE SYSTEM

The proposed crash avoidance circuit for a four-wheeled vehicle is shown in Fig. 2. The architecture of this neural network is based on a model of the cockroach escape circuit<sup>7</sup>. A sigmoidal function with bias is used to model the input-output relation of a neuron. The simulated vehicle is equipped with exteroceptors: 8 proximity sensors that are mounted on a horizontal ring around the vehicle such that its environment can be scanned. The measurements from all proximity sensors are fed forward to the ventral giant neurons and exteroceptive neurons. Apart from the measured information at current moment  $t$ , the radial measure of distance to an obstacle at the last sampling moment  $t-\Delta t$  is also recorded to infer the relative velocity and relative heading direction expressed with respect to the vehicle. The output of the exteroceptive neurons is the position of the obstacle relative to the vehicle normalized with respect to the maximum range of the proximity detector. The resulting data, distance ( $\underline{r}_0$ ) and heading ( $\underline{\theta}_0$ ), are transmitted to each thoracic interneuron.

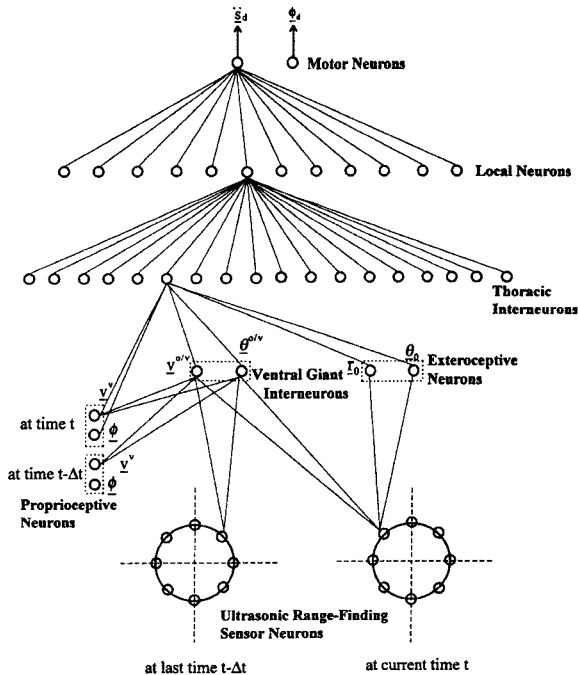


Figure 2: Crash avoidance system based on a neural network model of the cockroach escape circuit.

Proprioceptive neurons receive wheel speed data from simulated tachometers; the steering angle is also fed into the proprioceptive neurons. The outputs of the proprioceptive neurons are the speed of the vehicle  $\underline{v}^v$  and the steering angle each normalized with respect to their maximum values. The observed threat field, which is represented by the normalized magnitude of the velocity and normalized forward heading direction of an obstacle relative to the vehicle, is constructed by the outputs of ventral giant neurons (vGI). Ventral giant neurons receive the signals from the outputs of proprioceptive neurons and sensor neurons at the last sampling moment  $t-\Delta t$  and the current moment  $t$ .

The normalized speed and heading direction of the obstacle relative to the vehicle may be expressed as

$$\underline{v}^{o/v} = \frac{\sqrt{(v^o)^2 + (v^v)^2 - 2v^o v^v \cos(\theta^o - \theta^v - \alpha)}}{v_{\max}^v + v_{\max}^o}$$

$$\underline{\theta}^{o/v} = \frac{1}{2\pi} \tan^{-1} \left( \frac{v^o \sin(\theta^o - \theta^v) - v^v \sin \alpha}{v^o \cos(\theta^o - \theta^v) - v^v \cos \alpha} \right) \quad (8a,b)$$

where  $v^o$  and  $\theta^o$  are the speed and the heading direction of the moving obstacle;  $v_{\max}^v + v_{\max}^o$  denotes the maximum relative speed where the vehicle and moving obstacle travel in opposite directions.

Eighteen neurons reside in the thoracic layer and twelve neurons reside in the local layer. These numbers are chosen arbitrarily depending on the desired performance. Each thoracic interneuron receives a set of normalized data ( $\underline{v}^v, \underline{\phi}^v, \underline{v}^{o/v}, \underline{\theta}^{o/v}, \underline{r}_0, \underline{\theta}_0$ ) at the current moment  $t$ . Each neuron in the local layer connects with each neuron in the thoracic layer. The motor neurons receive the message from each local neuron. The outputs of the motor neurons are the avoidance commands expressed in the normalized tangential acceleration  $\underline{s}_d$  and normalized steering angle  $\underline{\phi}_d$  where

$$\underline{s}_d = 0.5 \left( 1 + \frac{\ddot{s}_d}{\ddot{s}_{\max}} \right); \quad \underline{\phi}_d = 0.5 \left( 1 + \frac{\phi_d}{\phi_{\max}} \right) \quad (9a,b)$$

The crash avoidance commands,  $\underline{s}_d$  and  $\underline{\phi}_d$ , are high level commands like those of the driver. These terms are transmitted to the controller to generate the low level signals. The desired tangential speed  $\dot{s}_d$  is set to be  $\dot{s}_d = \dot{s} + \ddot{s}_d \Delta t$ , where  $\Delta t$  is the sampling time. The desired steering angle speed and acceleration are set to zero after  $\Delta t$ .

The neural network was trained using back propagation to make the vehicle respond appropriately to potential crashes. The learning of this system is confined to varying the connection weights. In order to find the appropriate connection weights given the known structure

of the circuit, sufficient data are needed to train this system. These data were developed from a theoretical crash avoidance scheme.

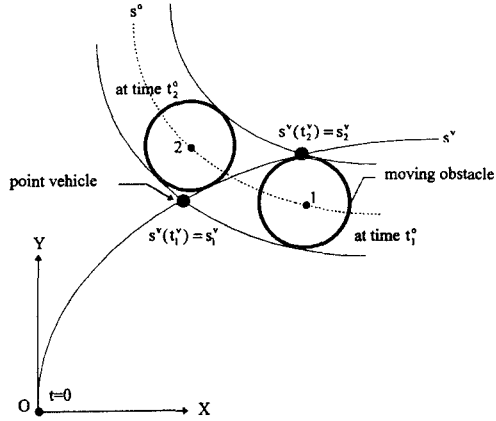


Figure 3: Crash alarm in a dynamic environment.

#### 4. CRASH AVOIDANCE SCHEME FOR TRAINING THE NEURAL NET

A crash alarm detection strategy is employed to derive a feasible crash avoidance behavior for training the neural network. As illustrated in Fig. 3, the vehicle is assumed to be contracted into a point and the obstacle is enlarged appropriately as a circle of radius  $R$ . The vehicle moves at constant speed  $v^v$  over a planned path  $s^v$  which is a function of time  $t$ ; the obstacle travels at speed  $v^o$ .

There is no knowledge of future obstacle motions in the real world, but only observations of the past and present obstacle motions which have been observed through the sensory systems. Therefore, for the purpose of crash alarm detection, we will treat the vehicle as following a straight path or a circular path at a constant speed  $v^v$ , and we will treat the moving obstacle as following a straight path at constant speed  $v^o$ .

Suppose that the vehicle arrives at the point  $s_1^v$  at time  $t_1^v$ , and passes through the impending crash site to the point  $s_2^v$  at  $t_2^v$ ; similarly, the center of the moving obstacle reaches position 1 and position 2 at time  $t_1^o$  and  $t_2^o$ , respectively, tangent to the trajectory  $s^v$  of the vehicle, a crash alarm set is defined as the following

$$\text{crash alarm set} := \{(v^v, s^v, v^o, s^o, R) \mid [t_1^v, t_2^v] \cap [t_1^o, t_2^o] \neq \emptyset; t_1^v > 0, t_2^o > 0\} \quad (10)$$

where  $t_1^v$  and  $t_2^v$  are defined to be larger than zero, because a negative  $t_1^v$  or  $t_2^v$  means that the vehicle or the obstacle has passed through the intersection. The crash

alarm set implies that the point vehicle will probably enter the circle and a crash will probably occur for the current state  $(v^v, s^v, v^o, s^o, R)$ .

When there is a crash alarm, avoidance actions are taken until the crash alarm set is no longer satisfied. The most desirable action is acceleration or deceleration. The acceleration scheme implies that the vehicle must pass through the intersection to  $s_2^v$  before the time  $t_1^o$ ; the deceleration scheme implies that the vehicle arrives at  $s_1^v$  at  $t \geq t_2^o$ . The conditions with a minimum acceleration or deceleration, respectively, for crash avoidance are

$$s_2^v = s^v(t_1^o); \quad s_1^v = s^v(t_2^o) \quad (11a,b)$$

The torque that causes the desired deceleration  $\ddot{s}^d$  or acceleration  $\ddot{s}^a$  and the corresponding tangential speed  $\dot{s}^d$  or  $\dot{s}^a$  at the points  $s_1^v$  and  $s_2^v$  must satisfy the constraints, Eqs. (4a,b). If there exists a feasible deceleration  $\ddot{s}^d$  and acceleration  $\ddot{s}^a$ , simultaneously, the desired tangential acceleration  $\ddot{s}_d$  will be chosen corresponding to the equation

$$\ddot{s}_d = \begin{cases} \ddot{s}^a & \text{if } \ddot{s}^a < -\ddot{s}^d \\ \ddot{s}^d & \text{otherwise} \end{cases} \quad (12)$$

If a feasible avoidance by acceleration/deceleration is not found along the pre-planned path because of constraints on acceleration or speed, turning from the planned path becomes necessary to avoid the crash. An iterative search is used to find the desired steering angle  $\phi_d$  which is closest to the current steering angle, while satisfying the constraints on the vehicle's performance.

#### 5. NUMERICAL EXAMPLES

##### 5.1 Training the neural network

Training cases were prepared using the crash avoidance scheme to train the neural network. The information  $(v^o, \theta^o, X^o, Y^o)$  of a moving obstacle and the current state  $(v^v, \theta^v, \phi, X^v, Y^v)$  of the vehicle are input to the crash avoidance scheme. If a crash alarm occurs during a sampling time  $\Delta t$ , the commands  $\ddot{s}_d$  and  $\phi_d$  will be generated and the torques,  $\tau_e$  and  $\tau_s$ , are synthesized and used as inputs to the vehicle simulation.

The training patterns are comprised of the training input data and output data and are generated per sampling time  $\Delta t$ , so each crash avoidance case will result in several training patterns. The neural network is trained using the back propagation method to find appropriate synaptic weights that will permit the vehicle to rapidly reproduce the crash avoidance motion.

The simulated vehicle travels over a straight path at a constant velocity  $\dot{s}=14$  m/sec in the heading direction  $\theta^v = \pi/2$ . The properties and performance limits of the vehicle are:  $m=1400\text{kg}$ ;  $I_z=2000\text{kgm}^2$ ;  $I_s=10\text{kgm}^2$ ;  $2a=2.5\text{m}$ ;  $2b=2\text{m}$ ;  $r_w=0.3\text{m}$ ;  $\dot{s}_{\max}=20\text{m/sec}$ ;  $\tau_{\max}=1200\text{Nm}$ ;  $\tau_{\min}=-1200\text{Nm}$ ;  $\phi_{\max}=\pi/6\text{rad}$ ;  $\phi_{\min}=-\pi/6\text{rad}$ ; the range of the proximity detector is  $D=50\text{m}$ ;  $\Delta t=0.5\text{sec}$ . The

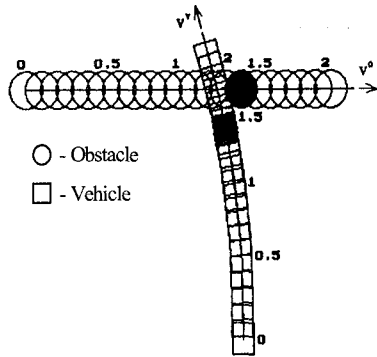


Figure 4: Crash avoidance for  $\theta^o = 0$ .

diagonal feedback gain matrices  $K_1$  and  $K_2$  are chosen as  $K_1 = \text{diag}[100,40]$  and  $K_2 = \text{diag}[0,800]$ .

An obstacle, modeled as a circle with radius  $R^o=1.5$  m, appears on the plane of motion moving at the constant speed  $v^o=14\text{m/sec}$  along a straight path. So the minimum distance between the obstacle and the vehicle is defined as  $R^o + \sqrt{a^2 + b^2} = 3.1$  m which is measured from the center of the moving obstacle to the c.m. of the vehicle.

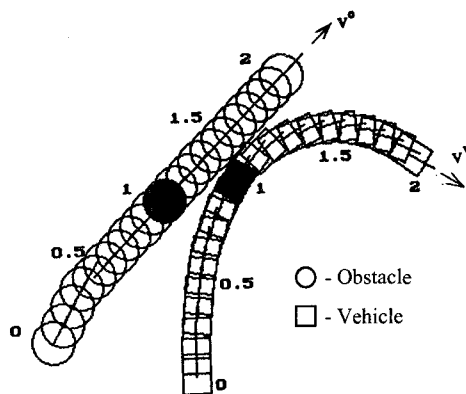


Figure 5: Crash avoidance trajectory as obstacle changes speed and direction.

An enlarged obstacle is employed in the crash avoidance scheme with a radius  $R=3.2\text{m}$ .

Using the crash avoidance scheme, the data used to train the neural network were gathered in simulation. Fourteen training cases were used each with a different

heading direction for the moving obstacle:  $0, \pi/6, \pi/4, \pi/3, 2\pi/3, 3\pi/4, 5\pi/6, \pi, 7\pi/6, 5\pi/4, 4\pi/3, 5\pi/3, 7\pi/4$  and  $11\pi/6$ .

Through a series of simulations using the 14 different cases, the data which represent the outputs of ventral giant interneurons, exteroceptive neurons, and proprioceptive neurons in this crash avoidance system constitute the training inputs; the desired commands are the outputs of motor neurons from the training outputs.

After the network was trained, the system was tested for the same 14 cases. Collisions occurred in a few cases. For those cases the second through the last sensed data were collected from the simulation and fed into the crash avoidance scheme to result in more training patterns. The system was then trained again to enhance the avoidance capability for the cases for which crashes occurred.

## 5.2 Crash Avoidance System Results

After the enhanced training, the performance of the system was tested again. All 14 crash situations were successfully avoided. The crash avoidance trajectory performed by the vehicle for  $\theta^o = 0$  is shown in Figure 4. The numbers (0, .5, 1, 1.5, 2) show the locations of the vehicle and obstacle at different times. The crash avoidance commands cause the vehicle to decelerate and steer left. The steering and braking torques closely follow those in the training case.

In order to test the flexibility of this system for an untrained case, the case for  $\theta^o=6\pi/5$  was used. The crash avoidance system was successful for this untrained case.

A moving obstacle may make an analogous avoidance maneuver so that the obstacle's behavior changes abruptly while the vehicle is avoiding a latent crash with the obstacle. Figure 5 shows the trajectory of the vehicle when the moving obstacle's heading direction changes from  $\theta^o=\pi/3$  to  $\theta^o=\pi/4$  and it slows from  $v^o=14$  m/sec to  $v^o=12$  m/sec at  $t=0.3$  second. The vehicle turns more sharply due to the unexpected behavior of the moving obstacle.

As a test of the cockroach-like context-dependent behavior, suppose that two moving obstacles threaten the vehicle's present situation. Obstacle 1, whose initial position is  $(20, \pi/4)$  in polar coordinates, moves at 14 m/sec with a heading of  $5\pi/4$ ; obstacle 2, whose initial position is  $(32, 11\pi/12)$ , moves at a speed of 11 m/sec with a heading of 0. At time zero, the vehicle travels at 14 m/sec with a heading of  $\pi/2$ , and its position is  $(20, 3\pi/2)$ .

At this instant, obstacle 1 is the more immediate threat. Figure 6 shows the crash avoidance trajectory of the vehicle for this situation. As the vehicle reflexively avoids the crash with obstacle 1, it also takes into account the impending collision with obstacle 2 in a context dependent manner and avoids both obstacles. Figure 7

shows the steering and engine torques during these avoidance maneuvers.

## 6. CONCLUSIONS

A model of a four wheeled vehicle with front wheel steering was developed. The simulated vehicle moves on a plane subject to the no-slip wheel constraint, a steering mechanism which prevents wheel scrub, and constraints on acceleration, speed and steering angle. The reduced nonlinear dynamic model has a controllability canonical form, permitting a smooth feedback linearization to be applied to design a controller for the vehicle. Proportional and derivative gains are chosen to decouple the system and assign eigenvalues corresponding to performance specifications.

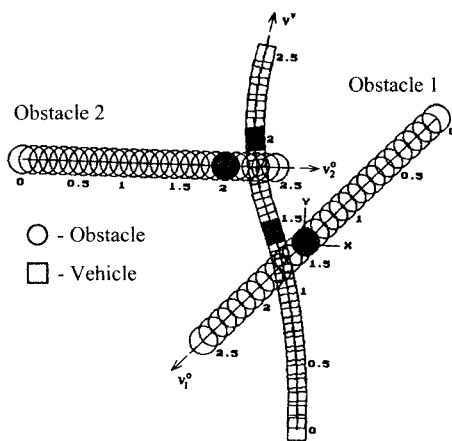


Figure 6: Vehicle avoiding two moving obstacles.

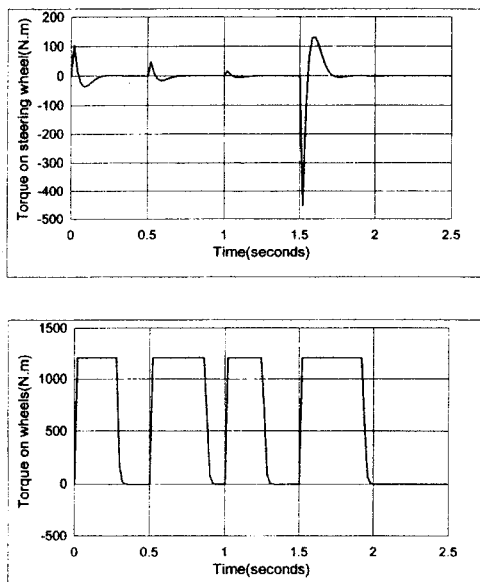


Figure 7: Steering and engine torques corresponding to Figure 6.

A neural network crash avoidance system similar in architecture to the escape system of the cockroach was developed for a wheeled vehicle. A crash avoidance scheme was derived to gather training data for the neural network. This scheme developed the desired commands such that the vehicle could successfully avoid a collision in a particular situation. However, the scheme takes time to be executed and, therefore, is not useful for on-line crash avoidance. The training of the neural network was conducted off-line in simulation. Simulations showed that the well trained crash avoidance system with the incorporation of context dependence is successful in causing the simulated vehicle to reflexively avoid impending collisions with multiple moving obstacles.

## Acknowledgements

This work was supported in-part by the Office of Naval Research Grant N00014-90-J-1545.

- <sup>1</sup> O. Khatib, "Real-Time Obstacle Avoidance for Manipulators and Mobile Robots," Proc. IEEE Int. Conf. Robotics and Automation, pp. 500-505, St. Louis, 1985
- <sup>2</sup> R. A. Brooks, "A robust Layered Control System for a Mobile Robot," IEEE Journal of Robotics and Automation, Vol. RA-2, No. 1, pp. 14-23, March, 1986.
- <sup>3</sup> J. Borenstein and Y. Koren, "The Vector Field Histogram - Fast Obstacle Avoidance for Mobile Robot," IEEE Transactions on Robotics and Automation, Vol. 7, No.3, pp. 278-288, June, 1991.
- <sup>4</sup> R. C. Arkin, "Modeling Neural Function at the Schema Level: Implications and Results for Robotic Control," In Biological Neural Networks in Invertebrate Neuroethology and Robotics. R.D. Beer, R.E. Ritzmann and McKenna eds. Academic Press, Chapter XVII, 1993.
- <sup>5</sup> D. Megherbi and W. A. Wolovich, "Real-time Velocity Feedback Obstacle Avoidance via Complex Variables and Conformal Mapping," Proceedings of the 1992 IEEE International Conference on Robotics and Automation, Nice, France, pp. 206-213, May, 1992.
- <sup>6</sup> R. E. Ritzmann, "The Neural Organization of Cockroach Escape and Its Role in Context Dependent Orientation," In Biological Neural Networks in Invertebrate Neuroethology and Robotics. R.D. Beer, R. E. Ritzmann and T. McKenna eds. Academic Press, Chapter VI, 1993.
- <sup>7</sup> R. D. Beer and H. J. Chiel, "Simulations of Cockroach Locomotion and Escape," In Biological Neural Networks in Invertebrate Neuroethology and Robotics. R. D. Beer, R. E. Ritzmann and McKenna eds. Academic Press, Chapter XII., 1993.
- <sup>8</sup> R. D. Beer, R. E. Kacmarcik, R. E. Ritzmann, and H. J. Chiel, "A Model of Distributed Sensorimotor control in the Cockroach Escape Turn," In Advances in Neural Information Processing Systems 3. R.P. Lippmann, J. Moody and D. S. Touretzky eds. Morgan Kaufmann, 1990.
- <sup>9</sup> J. Y. Wong, "Theory of Ground Vehicles," John Wiley & Sons, 1978.
- <sup>10</sup> C. Chen, "A Crash Avoidance System Based Upon the Cockroach Escape Response," Ph.D. dissertation, Case Western Reserve University, 1996.